

Elasticity of Stiff Polymer Networks

Jan Wilhelm and Erwin Frey

Hahn-Meitner-Institut, Abteilung Theorie, Glienicker Strasse 100, D-14109 Berlin, Germany
Fachbereich Physik, Freie Universität Berlin, Arnimallee 14, D-14195 Berlin, Germany

(Dated: April 30, 2018)

We study the elasticity of a two-dimensional random network of rigid rods (“Mikado model”). The essential features incorporated into the model are the anisotropic elasticity of the rods and the random geometry of the network. We show that there are three distinct scaling regimes, characterized by two distinct length scales on the elastic backbone. In addition to a critical rigidity percolation region and a homogeneously elastic regime we find a novel intermediate scaling regime, where the elasticity is dominated by bending deformations.

PACS numbers: 87.16.Ka, 62.20.Dc, 82.35.Pq

The elasticity of cells is governed by the cytoskeleton, a partially crosslinked network of relatively stiff filaments forming a several 100 nm thick shell called the actin cortex [1]. While the statistical properties of single cytoskeletal filaments are by now relatively well understood [2, 3], theoretical concepts for the elasticity of stiff polymer networks are still evolving. One major open question is to understand how stresses and strains are transmitted in such networks. In synthetic gels that are formed by rather flexible chain molecules the response to macroscopic external forces is – on the level of single filaments – isotropic and entropic in origin. It is generally believed that macroscopic stresses are transmitted in such a way that the local deformations within the network stay affine, i.e. that the end-to-end distance of individual filaments follows the macroscopic shear deformation [4]. In contrast, the building blocks of the actin cortex are semiflexible polymers, whose hallmark is an extremely long persistence length ℓ_p , which is comparable to the total contour length ℓ . As a consequence, the response of such stiff polymers to external forces shows a pronounced anisotropy [5]. Consider a semiflexible polymer with one end clamped at a fixed orientation. When forces are applied at the other end transverse to the tangent vector at the clamped end, the response may be characterized by a transverse spring coefficient $k_{\perp}(\ell) = 3\kappa/\ell^3$ proportional to the bending modulus κ . Whereas this response is of purely mechanical origin, the linear response for longitudinal forces is due to the presence of thermal undulations, which tilt parts of the polymer contour with respect to the force direction. The corresponding effective spring coefficient $k_{\parallel}(\ell) = 6\kappa^2/(k_B T \ell^4)$ is proportional to κ^2/T indicating the breakdown of linear response for very stiff filaments. In a typical network one expects the distance between crosslinks ℓ_c to be much smaller than the persistence length and filament length. Hence we have $k_{\parallel}(\ell_c)/k_{\perp}(\ell_c) = 2\ell_p/\ell_c \gg 1$, i.e. the elastic response of the filaments is indeed highly anisotropic.

These anisotropic elastic properties of individual filaments suggests that the macroscopic elasticity of networks will not only depend on the number of crosslinks and the

density of filaments, but also on the geometry and architecture of the network. For very regular networks such as a triangular lattice the longitudinal spring coefficient k_{\parallel} will dominate the macroscopic moduli [6] since the network can not be strained without a change of the end-to-end distance of individual polymers. In other regular network architectures, the softer bending modes would be dominant [7]. Naturally, this will lead to a very different prediction for the elastic modulus of the network. It is not at all obvious what type of network geometry (elongation dominated versus bending dominated) is relevant in less ideal structures with a significant amount of disorder such as in typical cytoskeletal networks.

As a first step towards understanding the elasticity of stiff polymer networks we consider a two-dimensional model defined as follows (see Fig. 1). We generate the

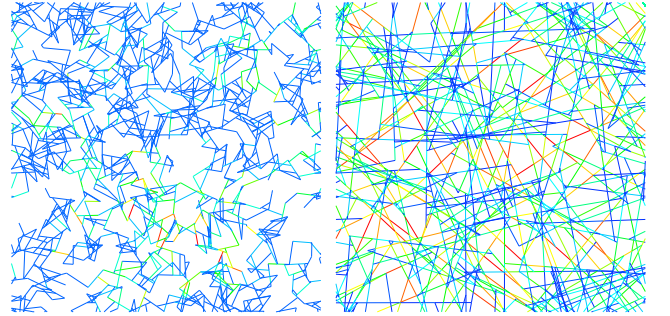


FIG. 1: Typical networks at low and high density. Dangling bonds, not contributing to the elasticity, have been cut off. The stress distribution is shown in false colors; the load on a filament increases from blue to red. The *left* picture is for $\rho = 10$, system size $L = 10$, and an aspect ratio $\alpha = 0.0001$. 99.99% of the strain energy stored in bending modes. In contrast, the *right* picture shows a network for $\rho = 50$, $L = 2$, and $\alpha = 0.01$, where only 5% of the strain energy is in bending modes; the remainder is stored in compression modes. For the choice of units see the main text.

random network by placing N line-like objects of equal length ℓ on a plane with area $A = L^2$ such that both position and orientation of the filaments are uniformly randomly distributed. Periodic boundary conditions in

both directions are used. Upon increasing the line density $\rho = N\ell/A$ there is a critical threshold ρ_c for geometric percolation [8]. Numerical simulations [9] show that the correlation length $\xi \sim (\rho - \rho_c)^{-\nu}$ of the incipient infinite percolation cluster scales with a critical exponent $\nu = 4/3$, identical to the value obtained for random site percolation on a lattice [10]. Transport of scalar quantities like the conductivity is also in the same universality class as lattice models [11]. In order to study the transport of non-scalar quantities like shear stress we need to specify how forces are transmitted between the building blocks of the network. In our “*Mikado model*” the building blocks are homogeneous elastic rods characterized by a Young modulus E and a circular cross-section of radius r . Wherever two sticks intersect they are connected by a crosslink with zero extensibility. In the cytoskeleton one finds a variety of linker proteins with a range of mechanical properties [12]. Here we restrict ourselves to crosslinks that either fix the relative orientation of the rods (“stiff crosslinks”) or allow free rotation (“free hinges”). Similar to thermally fluctuating semiflexible polymers, the elastic response of a stick segment between two neighboring crosslinks is characterized by length dependent force constants for compression or elongation, $k_{\text{comp}}(\ell_c) = \pi r^2 E / \ell_c$, and bending, $k_{\text{bend}}(\ell_c) = k_{\perp}(\ell_c) = (3/4)\pi r^4 E / \ell_c^3$. The distance between two crosslinks ℓ_c shows a Poissonian distribution, where the average distance of crosslinks along a filament scales as the inverse of the line density, $\bar{\ell}_c = \pi / \rho$ [8]. While this is a purely mechanical model, it still captures the essential feature that for typical densities of the network the compressional stiffness is much larger than the bending stiffness, $k_{\text{comp}}(\ell_c) / k_{\text{bend}}(\ell_c) = (4/3)\ell_c^2 / r^2 \gg 1$. It leaves out steric effects due to thermal fluctuations of the filaments, which give rise to the plateau modulus in solutions [13].

Consider the energy of the network as a function of the deviations of the positions of all intersection points and the rod orientations at the intersection points from their initial values. For small deformations of the network, this function can be approximated by a quadratic form that vanishes for vanishing deviations, as—by construction—the undeformed network is not prestressed. To analyse the elastic properties of the model network, a shear deformation respecting the periodic boundary conditions is enforced by demanding that corresponding points on the left and right boundary of the simulation cell undergo equal displacements while the displacements of corresponding points on the upper and lower boundary of the cell must agree vertically but differ horizontally by a distance $\Delta = \gamma L$, where γ is the shear strain. The orientation of the rods at corresponding points on the boundary are required to be equal. The remaining degrees of freedom are then allowed to relax, i.e. the harmonic approximation to the energy of the network is minimized in the presence of the constraints. The derivative of the

resulting energy of the deformed state with respect to the strain γ is proportional to the shear modulus. In principle, this reduces the determination of the shear modulus of a given network to the solution of a linear equation. However, for interesting parameters (thin rods), the problem is numerically highly unstable as we are searching for the lowest point of a complicated high-dimensional valley with extremely steep slopes but hardly varying base altitude. This problem is best left to one of the commercially available finite element solvers which have seen many years of careful optimization and testing. The results presented below were obtained using the program Nastran by MSC Software.

In the following discussion we take the rod length ℓ as unit length and κ / ℓ^3 as unit for the elastic modulus. Then the independent parameters are the density ρ , the system size L and the aspect ratio $\alpha = r / \ell$ of the rods. Note that the latter is a measure of the relative magnitude of compressional to bending stiffness.

We start with an analysis of the elasticity close to the percolation threshold. For stiff crosslinks we find that the percolation threshold is the same for rigidity as for connectivity percolation, $\rho_c = 5.71$. For free hinges a higher line density of filaments is needed, $\rho_c = 6.7$, for the network to become rigid. This agrees well with recent results, $\rho_c = 6.68$, for stiff fiber networks [14], where the crosslinks are fixed in space but the angles between the fibers can vary. In both cases, we find that the shear modulus G vanishes as the line density of sticks approaches the critical value ρ_c , according to a power law $G \sim (\rho - \rho_c)^\mu$. For our numerical analysis on a finite lattice we expect the shear modulus to obey the following finite size scaling law

$$G = L^{-\mu/\nu} h(L/\xi), \quad (1)$$

where the scaling function behaves as $h(x) \sim x^{\mu/\nu}$ and $h(x) \sim 1$ for large and small values of the scaling variable $x = L/\xi$, respectively. Fig. 2 shows that the data collapse works very well for densities ranging from values close to the percolation threshold ρ_c up to $\rho \approx 20$. For the data shown, L ranges from 2 to 30. For larger densities, systematic deviations are clearly visible. This will turn out to be a very interesting observation, as we will discuss in detail below. We get the best data collapse in the critical region if we choose the values 2.4 ± 0.2 and 2.3 ± 0.2 for the critical exponent μ/ν in the case of stiff crosslinks and free hinges, respectively. Since the difference between the exponents is within the statistical error, we can make no definite conclusion whether networks with free hinges and stiff crosslinks belong to different universality classes for elasticity percolation.

The rigidity exponent $\mu \approx 3.15 \pm 0.2$ is significantly lower than in other classes of continuum percolation models, like the “Swiss-cheese model”, where $\mu \approx 5$ [15, 16]. It is also lower than the value $\mu \approx 4$ for lattice models with bond-bending forces [10, 17]. Hence it seems likely

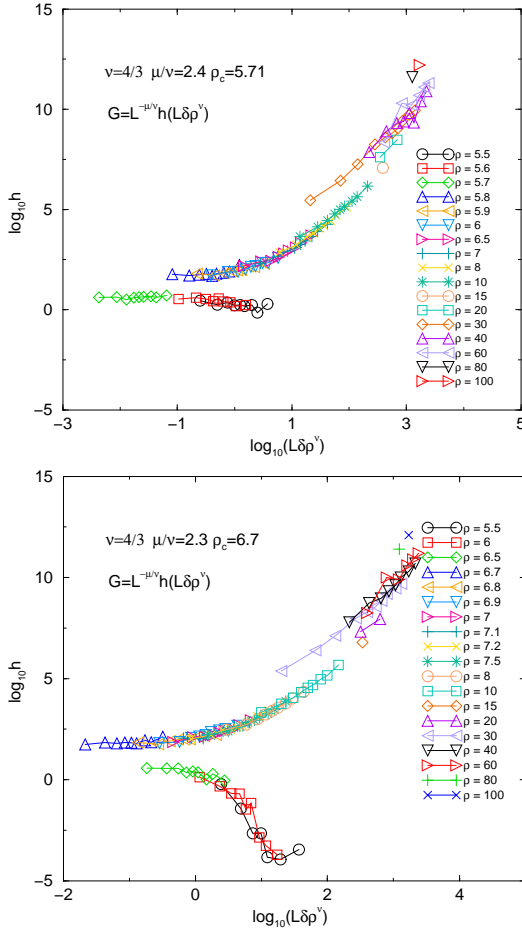


FIG. 2: Double logarithmic plot of the scaling function $h(x)$ for the shear modulus of the “Mikado model” with stiff crosslinks (top) and free hinges (bottom) as a function of $x = L|\delta\rho|^\nu$ with $\delta\rho = \rho - \rho_c$ for a series of densities ρ indicated in the graphs. Note that for finite systems the shear modulus is also nonzero below ρ_c (lower branches in both plots).

that the “Mikado model” constitutes a new universality class for rigidity percolation. Similar results have independently been found in Ref. [18].

Now we come back to the above mentioned systematic deviations from the scaling law, Eq. 1, at densities above $\rho \approx 20$. To understand these better, let us have a closer look at the shear modulus as a function of the elastic moduli of individual filaments for densities not too close to the percolation threshold. In this regime the shear modulus becomes independent of system size for moderately large systems; for the following results we have chosen systems satisfying $L/\xi \geq 200$. Fig. 3 shows the shear modulus as a function of α for a series of densities; we have communicated a preliminary version of these data in Ref. [19]. Note that $k_{\text{bend}}(\ell)$ is effectively kept constant since we are measuring all

elastic constants in units of κ/ℓ^3 . There are two strik-

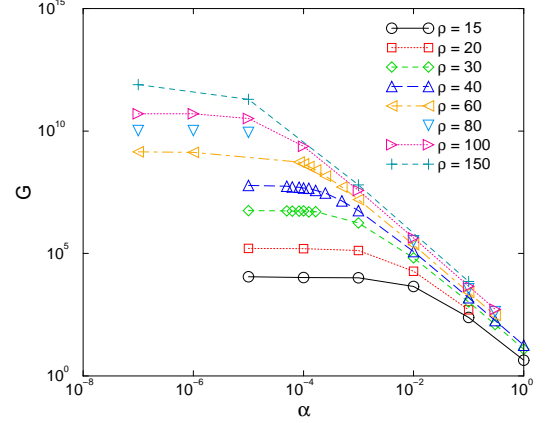


FIG. 3: Double logarithmic plot of the shear modulus G as a function of α for fixed $k_{\text{bend}}(\ell)$. Data are shown for free hinges.

ingly different regimes. For high densities and/or thick rods ($\alpha \gtrsim 0.1$), where compressional stiffness is lower or comparable to the bending stiffness (lower right part of Fig. 3), the shear modulus scales linearly with the filament compressional modulus and the number of filaments per unit area, $G \sim (\rho - \rho_c)\alpha^{-2}$. Such a linear regime has also been found in a series of studies on random fiber networks [20]. It is by now well established that the elastic modulus can be described quantitatively in terms of effective medium models [21]. Hence, in the high line density regime the network behaves as a homogeneously elastic medium, dominated by the compressional modulus of the individual filaments. As a consequence, local deformations follow a macroscopic shear in an affine way. This has to be contrasted with the elastic behavior for slender rods with low aspect ratios ($\alpha \approx 10^{-5}$ for the higher densities), where bending becomes the softer mode. Then, one finds an extended plateau region, which broadens significantly with lowering the line density, where the shear modulus becomes completely independent of $k_{\text{comp}}(\ell) \sim \alpha^{-2}k_{\text{bend}}(\ell)$ [19]. This strongly suggests that in this regime the macroscopic elasticity of the network is dominated by bending stiffness of individual filament. This conclusion is corroborated by the observation that almost all of the energy stored in the deformed network is accounted for by transverse deformation of the rods (compare Fig. 1). Another remarkable feature of this plateau regime is the strong dependence of the shear modulus on line density. We find $G \sim (\rho - \rho_c)^{\mu'}$ with a rather large exponent $\mu' \approx 6.7$. From the above analysis it may seem as if the anomalous elasticity in the plateau regime and the homogeneous elasticity in the affine regime are two separate phenomena, and one might wonder how one emerges from the other. To analyze this

relation we try a crossover scaling ansatz,

$$G = (\rho - \rho_c)^{\mu'} g[\alpha(\rho - \rho_c)^{\nu'}] = \xi'^{-\mu'/\nu'} \tilde{g}(\alpha/\xi'), \quad (2)$$

where we have defined a new length scale $\xi' \sim (\rho - \rho_c)^{-1/\nu'}$. For this ansatz to reduce to the modulus expected in the affine region, the scaling function $g(x)$ needs to scale as $g(x) \sim x^{-2}$ for $x \gg 1$ and the exponents need to obey the scaling relation $\mu' = 2\nu' + 1$. In the plateau regime, $g(x)$ is expected to be constant. As shown in Fig. 4, we obtain an excellent scaling collapse for over almost eight orders of magnitude in the scaling variable $x = \alpha/\xi'$ using $\nu' = 2.83$ or equivalently $\mu' = 6.67$ and the critical line density $\rho_c \approx 5.71$, associated with connectivity percolation. Additionally, the scaling function $g(x)$ displays the expected behavior. Meeting both of these requirements is highly nontrivial, and gives strong evidence for the anomalous scaling law in Eq. 2.

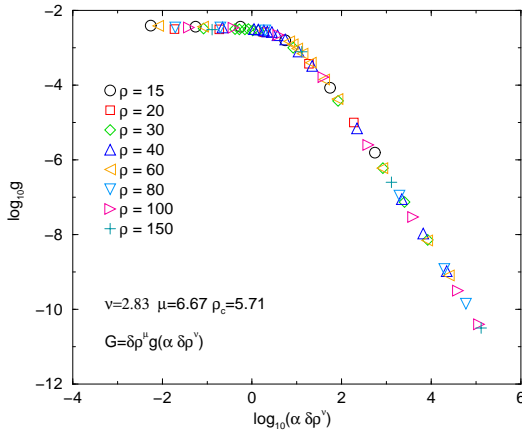


FIG. 4: Scaling plot of the shear modulus for free hinges for a series of densities above $\rho = 15$ indicated in the graph (same data as in Fig. 3). Data collapse to the crossover scaling form, Eq. 2, is obtained with $\nu' = 2.83$. Note that here and in all other figures the unit of length is ℓ and the unit of the shear modulus G is κ/ℓ^3 .

The existence of such a broad scaling regime far from the percolation threshold is a surprising and intriguing feature of stiff polymer networks. At the moment we are lacking a complete understanding of its physical origin. In particular, the geometrical significance of the new length scale ξ' remains unclear. One may speculate that the anomalous scaling behavior is a subtle consequence of the interplay between quenched randomness of the network structure and long-range correlation effects induced by the stiffness of the filaments. An immediate consequence of the scaling form, Eq. 2, is the existence of a crossover line density ρ_{cross} scaling as $\ell \rho_{\text{cross}} \sim \alpha^{-1/\nu'}$, where we have re-introduced units of length ℓ . This implies that increasing filament length at constant line density drives the system towards the affine regime, in accord with Ref. [18].

While these results for an idealized two-dimensional model are certainly not straightforwardly applicable to three-dimensional cytoskeletal networks, one may still try to get an idea for the scales involved. We expect that network densities can be compared roughly by using the average distance ℓ_c between intersections as a measure: A cytoskeletal network might have $\ell_c \approx 0.1 \mu\text{m}$ with typical filament lengths of $2 \mu\text{m}$. These values correspond to a two-dimensional line density of $\rho \approx 20$ and an aspect ratio of $\alpha \approx 0.002$, which would place a typical actin network in the bending dominated intermediate regime.

Understanding the full complexity of cytoskeletal networks certainly merits further theoretical and experimental work. Building on the knowledge gained from our idealized model, future investigations may among many other questions want to address three-dimensional systems, polydispersity, thermal fluctuations or even the kinetics of the crosslinking molecules.

We acknowledge M. Alava and K. Kroy for useful discussions and comments, and P. Benetatos for a critical reading of the manuscript.

-
- [1] B. Alberts *et al.*, *Molecular Biology of the Cell*, 3 ed. (Garland Publ., New York, 1994).
 - [2] J. Wilhelm and E. Frey, *Phys. Rev. Lett.* **77**, 2581 (1996).
 - [3] L. LeGoff, O. Hallatschek, E. Frey, and F. Amblard, *Phys. Rev. Lett.* **89**, 258101 (2002).
 - [4] M. Doi and S. F. Edwards, *The Theory of Polymer Dynamics* (Clarendon Press, Oxford, 1986).
 - [5] K. Kroy and E. Frey, *Phys. Rev. Lett.* **77**, 306 (1996).
 - [6] F. MacKintosh, J. Käs, and P. Janmey, *Phys. Rev. Lett.* **75**, 4425 (1995).
 - [7] R. Satcher, and C. Dewey, *Biophys. J.* **71**, 109 (1996).
 - [8] G. Pike and C. Seager, *Phys. Rev. B* **10**, 1421 (1974).
 - [9] Y. Leroyer and E. Pommiers, *Phys. Rev. B* **50**, 2795 (1994).
 - [10] D. Stauffer and A. Aharony, *Introduction to Percolation Theory*, 2 ed. (Taylor & Francis, London, 1994).
 - [11] I. Balberg, N. Binenbaum, and N. Wagner, *Phys. Rev. Lett.* **52**, 1465 (1984).
 - [12] L. Limozin and E. Sackmann, *Phys. Rev. Lett.* **89**, 168103 (2002).
 - [13] B. Hinner *et al.*, *Phys. Rev. Lett.* **81**, 2614 (1998).
 - [14] M. Latva-Kokko and J. Timonen, *Phys. Rev. E* **64**, 066117 (2001).
 - [15] S. Feng, B. I. Halperin, and P. N. Sen, *Phys. Rev. B* **35**, 197 (1987).
 - [16] L. Benguigui, *Phys. Rev. B* **34**, 8176 (1986).
 - [17] S. Arbabi and M. Sahimi, *Phys. Rev. B* **47**, 703 (1993).
 - [18] D. A. Head, A. J. Levine, and F. C. MacKintosh, cond-mat/0303499.
 - [19] E. Frey, K. Kroy, J. Wilhelm, and E. Sackmann, in *Dynamical Networks in Physics and Biology*, edited by G. Forgacs and D. Beysens (Springer Verlag, Berlin, 1998).
 - [20] V. Räsänen, M. Alava, K. Niskanen, and R. Nieminen, *J. Mater. Res.* **12**, 2725 (1997).
 - [21] J. Åström *et al.*, *Phys. Rev. E* **61**, 5550 (2000).